Hindawi
Wireless Communications and Mobile Computing
Volume 2019, Article ID 1914762, 11 pages
https://doi.org/10.1155/2019/1914762

WILEY | Hindawi

Research Article

Performance Analysis for Downlink MIMO-NOMA in Millimeter Wave Cellular Network with D2D Communications

Jianguo Li, Xiangming Li, Aihua Wang, and Neng Ye

School of Information and Electronics, Beijing Institute of Technology, Beijing, China

Correspondence should be addressed to Xiangming Li; xmli@bit.edu.cn

Received 4 April 2019; Accepted 3 June 2019; Published 19 June 2019

Guest Editor: Xi Chen

Enabling nonorthogonal multiple access (NOMA) in device-to-device (D2D) communications under the millimeter wave (mmWave) multiple-input multiple-output (MIMO) cellular network is of critical importance for 5G wireless systems to support low latency, high reliability, and high throughput radio access. In this paper, the closed-form expressions for the outage probability and the ergodic capacity in downlink MIMO-NOMA mmWave cellular network with D2D communications are considered, which indicates that NOMA outperforms TDMA. The influencing factors of performance, such as transmission power and antenna number, are also analyzed. It is found that higher transmission power and more antennas in the base station can decrease the outage probability and enhance the ergodic capacity of NOMA.

1. Introduction

With the rapid growth of a variety of 5th-generation wireless systems commercial requirements, like 8k video, cloud VR, unmanned driving, smart city, etc., the demands on high data rates, low latency, and high reliability of wireless communication are increasing rapidly. As the core technologies of 5G, the wide bandwidth and large scale antenna arrays can be used by mmWave MIMO to provide high data rates. Meanwhile, NOMA can increase the spectral efficiency of transmission so that more data is transmitted over the same bandwidth spectrum. At the same time, due to the short communication distance, D2D communication can obtain lower transmission power and lower delay to ensure the battery availability and system reliability. Therefore, combined with MIMO-NOMA and mmWave in D2D communications, the throughput of the entire cell system can be improved.

D2D communication was noticed as a viable candidate for some certain applications such as proximity services, content sharing, multiparty games, and coverage discovered with business purposes in the 3rd-Generation Partnership Project (3GPP) Long-term Evolution (LTE) 12th and 13th editions [1, 2]. By sharing the same resource blocks with downlink cellular users, D2D communication is a useful technology which can enhance the spectrum efficiency and system capacity successfully. Due to the short communication distance, D2D pairs can communicate with each other directly without being relayed by the base station which can reduce transmission power, increase transmission reliability, and extend system range [3, 4]. Since the cellular user and the D2D user coexist, if the D2D user and the cellular user are not well coordinated, it will not bring any benefits and may affect the communication of the normal cellular user. According to the literature [5], based on the overlapping coalition formation game theory, the authors have proposed a method to conduct joint interference management and resource allocation in the D2D communications. In addition, a new interference management strategy has been discussed to enhance the overall sum rate of cellular networks and D2D pairs which has combined the conventional mechanism and δ_D-interference limited area control scheme [6]. Furthermore, a graph theoretic approach for transmission-order optimization scheme in bidirectional D2D communications underlaying cellular TDD networks has been introduced in the [7]. Meanwhile, the authors in [8] have considered a continuous beamforming vector design for all cellular users and the D2D pairs association vector search algorithm to maximize the capacity of the cellular users and D2D pairs. In order to reduce the interference between the cellular users and D2D pairs, a combining call admission control and power

control scheme under guaranteeing QoS of every users in the cellular network has been presented in [9]. Besides, it is significant that the NOMA and MU-MIMO can also improve the overall system throughput in the cellular network with underlaid D2D communications, which have been proposed in [10].

As the core technology of 5G, NOMA can serve multiple users in the same resource block, such as a time slot, frequency channel, or spreading code. Compared to the orthogonal multiple access, NOMA can provide a set of visible benefits such as greater spectrum efficiency and higher system throughout [11–15]. There are two available NOMA technology categories, namely, power-domain and code-domain NOMA, widely used in the cellular network. This paper focuses on the power-domain NOMA which divides the users in power-domain. On the transmitter sides, signals from multiple users are transmitted at the same resource blocks. On the receiver sides, the multiuser detection algorithms, such as successive interference cancellation, have been utilized to detect the signal, regarding the weak signal as the interference, and decode the strong signal while cancelling the strong signal to detect the weak signal [16, 17]. Aiming at enhancing system capacity and user fairness, the authors have presented a novel resource and power allocation technique which can provide a flexible balancing between capacity and fairness maximization in [18]. Meanwhile, the optimum received power levels of uplink NOMA signal have been proposed in [19]. Furthermore, comparing with OMA in massive connectivity, NOMA can supply more users than OMA because of the limited number of supported users by the amount of the available resources [20–22]. In addition, the analytical outage probability expression for each user has been derived in the downlink cooperative NOMA network over Nakagami-m fading channels in [23]. Since the perfect channel state information at the transmitter side is nearly impractical for many communication scenarios, the literature [24] presented a practical downlink NOMA system over the Nakagami-m fading channels with statistical CSI associated with each other. At the same time, the authors attempted to combine the NOMA and MIMO to accomplish high spectral efficiency [25, 26]. Additionally, the outage probability of the massive MIMO-NOMA system has been derived with perfect user-ordering and limited feedback [27]. Besides, the scheme discussed in [28] required that the number of antennas at the receiver is larger than that at the transmitter instead of the CSI at the transmitter. In [29], the optimal and low complexity suboptimal power allocation schemes have been proposed to maximize the ergodic capacity of MIMO-NOMA system with statistical channel state information in the transmitter over Rayleigh fading channel. Also, the authors in [30] have proposed a cluster beamforming strategy which can optimize beamforming vectors and power allocation coefficients in MIMO-NOMA system to decrease the total power. In addition, NOMA can improve the achievable rate greatly in the D2D-aided cooperative relaying system in the literature [31].

Nowadays, as spectrum resources become increasingly scare, the mmWave band with a wider spectrum becomes a natural choice for large-volume content services [32]. Meanwhile, benefitting from the small wavelength of mmWave, the large scale antenna arrays can be adopted easily. Combining the high gain directional antenna and beamforming technology enabled by massive antennas, the high data rates can be reached within a 200-meter mmWave cellular network which has high path loss in mmWave band [33]. In the literature [34], the authors have proposed that the base station which is equipped with a large antenna array can serve a set of users through the users precoding with massive MIMO. Furthermore, the literature [35] has proved that the orders of magnitude are increased in spectral efficiency with massive MIMO which can offer more multiuser gain. However, as for MIMO in conventional cellular frequency band, the beamforming precoding is totally achieved in the digital domain which can cancel the interference between different beams. In order to realize the precoder in the digital domain, a dedicated RF chain is needed by every antenna. But it is difficult for the mmWave base station with large scale antennas whose energy consumption is a large part of the total energy consumption at mmWave frequencies due to the wide bandwidth [36]. At the same time, the authors in [36] have discussed a successive interference cancellation-based hybrid precoding method with near-optimal performance and low complexity which can maximize the achievable subrate of each subantenna array and avoid the need for singular value decomposition and matrix inversion. Additionally, the literature [37] has proposed an interference-aware beam selection which can avoid serious multiuser interferences to reduce obvious performance loss. Besides, the authors in [38] have proposed a practical design of hybrid precoders and combiners with low-resolution phase shifters in mmWave MIMO systems adopting an iterative algorithm for hybrid precoders and combiners to optimize the spectral efficiency. Moreover, the MIMO capacity has been computed over the Nakagami-m fading channel in [39] and the closed-form expressions for outage probabilities achieved by NOMA users in a multicell downlink mmWave network have been obtained over a Poisson cluster point process. Moreover, a fine-grained performance analysis over Poisson bipolar model of the mmWave D2D communication networks was provided in [40]. The literature [41] has presented an in-depth capacity analysis for the integrated NOMA mmWave-massive-MIMO systems which can achieve significant capacity improvements.

Because of the large link attenuation and weak coverage in the MIMO-NOMA cellular network, the D2D communication can be used to enhance service for cell edge users. In this paper, the outage probability and the ergodic capacity are proposed in the downlink MIMO-NOMA cellular network with D2D communications. The remaining part of this paper is organized as follows. In Section 2, we introduce a system model of the downlink MIMO-NOMA cellular network with multiple direct D2D pairs underlaying communication. The closed-form expressions of the performance analysis including the outage probability and the ergodic capacity are given in Section 3. Finally, the numerical results in Section 4 validate the theoretical analysis and demonstrate that the system capacity can be improved by the integrated MIMO-NOMA in the mmWave network with D2D communications.

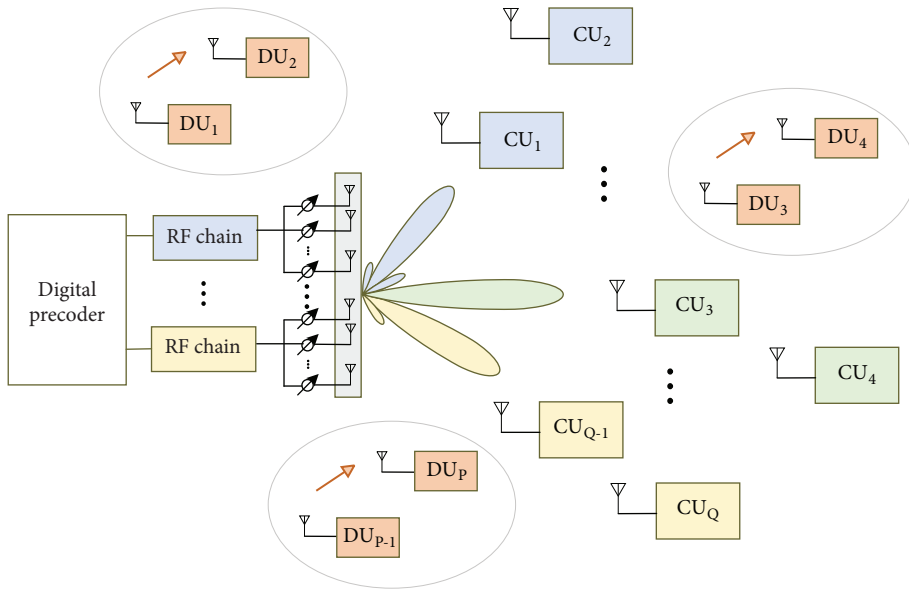

FIGURE 1: System model of D2D-aided mmWave MIMO-NOMA.

2. System Model

The paper considers a downlink NOMA, MU-MIMO mmWave cellular network with multiple direct D2D pairs underlaying communications where the cellular users are randomly distributed. The same mmWave resources are used by the cellular user and D2D pairs with NOMA. The mmWave MIMO-NOMA D2D communication system model is shown in Figure 1. The base station is equipped with multiple antennas, which can generate high directional and high gain beams for cellular users. There are Q cellular users with signal antenna and P D2D users with signal antenna in the cellular network, which are denoted as $CU_1, CU_2, \ldots, CU_Q$ and $DU_1, DU_2, \ldots, DU_P$. The D2D pairs are randomly distributed in the edge of the cellular network and there is no direct link between the base station and the D2D pairs [10].

2.1. NOMA Signal. In beam n, we assume that $u(n,1)$, $u(n,2)$, ..., $u(n,K)$ are scheduled on the same radio resource with NOMA, $K \geq 2$, where CU of k_{th} in the beam n is denoted as $u(n,k)$. x_n is the transmitted signal by the base station in the beam n, which is the sum of all K user signals.

$$x_n = \sum_{i=1}^{K} \sqrt{\lambda_{u(n,i)} P_n} S_{u(n,i)}, \tag{1}$$

where $\lambda_{u(n,k)}$ is the power ratio of k_{th} user, $\|\lambda_{u(n,1)}\| \leq \|\lambda_{u(n,2)}\| \leq \|\lambda_{u(n,K)}\|$, and $\sum_{k=1}^{K} \lambda_{u(n,k)} = 1$. P_n is the total power in the beam n, $S_{u(n,k)}$ is the normalized transmitted signal of k_{th} user in the beam n, and $\mathbb{E}(\|S_{u(n,k)}\|^2) = 1$.

2.2. Channel Model. As for the large scale fading, the mmWave link is similar to that used in [33]; the large scale fading $L(r)$, in dB, is modeled as

$$L(r) = \rho + 10\alpha \log(r), \tag{2}$$

where $\rho = 32.4 + 20\log(f_c)$, f_c is the carrier frequency, α is the path loss exponents, and r is the distance from transmitter to receiver.

As for the small scale fading, the Nakagami-m fading is considered for each link. $h_{u(n,k)}, h_{pu(n,k)}, h_{p'p}$ are donated as the link of base station to cellular user, D2D user to cellular user, and D2D user to D2D user whose modular square is normalized Gamma random variable [39]. And when H is normalized Gamma random variable, which is denoted as $H \sim Gamma(\omega, \psi)$, the probability density function $f(x)$ and Cumulative Distribution Function $F(x)$ of H are

$$f(x) = \frac{1}{\psi^{\omega}\Gamma(\omega)} x^{\omega-1} e^{-x/\psi}, \tag{3}$$

$$F(x) = \begin{cases} 1 - \sum_{J=0}^{\omega-1} \frac{1}{j!\psi^j} x^j e^{-x/\psi}, & x \geq 0 \\ 0, & \text{otherwise.} \end{cases} \tag{4}$$

2.3. Directional Beamforming. The base station with mmWave band is equipped with multiple antennas which can generate high directional and high gain beams. The actual antenna pattern is modeled as the sectorized antenna model approximately for the sake of mathematical tractability [42]. Generally the maximum power gain is adopted to replace the array gain within the half-power beam width (main lobe gain), and the first minor maximum gain is used to replace the gains of the other DoAs (side lobe gain). According to the literature [39, 40], when the antenna pattern is a planar square, the total array gain from base station to the user is $G_{(n,k)}$ where

$$G_{(n,k)} = \begin{cases} T, & mainlobe \\ \tau, & sidelobe, \end{cases} \tag{5}$$

where $T = L$, $\tau = 1/\sin^2(3\pi/2\sqrt{L})$ and L is the number of antennas.

2.4. Received Signal. For downlink MIMO-NOMA transmission, the cellular user $u(n, K)$ will receive the sum of signal from base station and the signal from D2D transmitter at the same time. In addition to receiving the D2D transmitted signal, the D2D receiver DU_P will also receive the interference signal from the other D2D users. Without loss of generality, we assume there are N beams and M D2D pairs in the cellular network; then the received signal of cellular user $y_{u(n,k)}$ and the received signal of D2D user y_{D_p} can be formulated as

$$y_{u(n,k)} = h_{u(n,k)} \sum_{n=1}^{N} G_{(n,k)} x_n + \sum_{p=1}^{M} \sqrt{P_D} h_{pu(n,k)} S_p + n_{u(n,k)}, \quad (6)$$

$$y_{D_p} = \sum_{p'=1}^{M} \sqrt{P_D} h_{p'p} S_{p'} + n_{D_p}, \quad (7)$$

where $h_{u(n,k)}$ is the channel gain for downlink $u(n, K)$, $\|h_{u(n,1)}\| \geq \|h_{u(n,2)}\| \geq \|h_{u(n,K)}\|$, $h_{pu(n,k)}$ is the channel gain between DU_P and $u(n, K)$, and $h_{p'p}$ is the channel gain from $DU_{p'}$ transmitter to DU_p receiver. $G_{(n,k)}$ is the total beamforming array gain from base station to $u(n, K)$. x_n is the superimposed signal by the total K $u(n, k)$ in the beam n. P_D is the transmitted power of DU_P. S_p is the signal transmitted by DU_P, and $\mathbb{E}(\|S_p\|^2) = 1$. Meanwhile $n_{u(n,k)}$ and n_{D_p} are the i.i.d. white Gaussian noise with zero mean and one variance at cellular user $u(n, k)$ and D2D user DU_P, which is denoted as $n_{u(n,k)}, n_{D_p} \sim \mathcal{C}N(0, 1)$.

We denote the SINRs of $u(n, k)$ and DU_P in the downlink NOMA-MIMO cellular network as $\gamma_{u(n,k)}$, γ_{DU_p}. Without loss of generality, the interbeam interference is ignored in this paper. In the meantime, the perfect SIC is used to prevent error propagation in the NOMA users in the paper. Using (1) in (6) and (7), $\gamma_{u(n,k)}$ and γ_{DU_p} can be formulated as

$$\gamma_{u(n,k)} = \frac{\lambda_{u(n,k)} P_n \left\| h_{u(n,k)} G_{(n,k)} \right\|^2}{I^N_{u(n,k)} + I^D_{u(n,k)} + \sigma_n^2}, \quad (8)$$

$$\gamma_{D_p} = \frac{P_D \left\| h_{pp} \right\|^2}{I^D_{D_p} + \sigma_n^2}, \quad (9)$$

where

$$I^N_{u(n,k)} = \sum_{k'=1}^{k-1} \lambda_{u(n,k')} P_n \left\| h_{u(n,k)} G_{(n,k)} \right\|^2, \quad (10)$$

$$I^D_{u(n,k)} = \sum_{p'=1}^{M} P_D \left\| h_{p'u(n,k)} \right\|^2, \quad (11)$$

$$I^D_{D_p} = \sum_{p'=1, p' \neq p}^{M} P_D \left\| h_{p'p} \right\|^2. \quad (12)$$

3. Performance Analysis

In this section, we present the performance analysis of D2D-aided mmWave MIMO-NOMA system. Specifically, the closed-form expressions for the performance metrics (i.e., the outage probability and the ergodic capacity) are presented in the following. Without loss of generality, in the beam n, k-th *CUs* are adopted with NOMA in one beam, $k \in \{1, 2\} \|h_{u(n,1)}\| \geq \|h_{u(n,2)}\|$, and one *DU* is randomly distributed at the edge of the beam. Three events are considered in this system.

Event 1. According to the NOMA successive interference cancellation (SIC) principle, user 1 obtains the information intended for user 2 with $\gamma_{1 \longrightarrow 2}$ and removes it. When decoding the information intended for user 2, user 1 cancels it successfully with γ_1.

$$\gamma_{1 \longrightarrow 2} = \frac{\lambda_{u(n,2)} P_n \left\| h_{u(n,1)} G_{(n,1)} \right\|^2}{\lambda_{u(n,1)} P_n \left\| h_{u(n,1)} G_{(n,1)} \right\|^2 + P_D \left\| h_{pu(n,1)} \right\|^2 + \sigma_n^2}, \quad (13)$$

$$\gamma_1 = \frac{\lambda_{u(n,1)} P_n \left\| h_{u(n,1)} G_{(n,1)} \right\|^2}{P_D \left\| h_{pu(n,1)} \right\|^2 + \sigma_n^2}. \quad (14)$$

Event 2. User 2 decodes the signal with γ_2, treating user 1 as interference.

$$\gamma_2 = \frac{\lambda_{u(n,2)} P_n \left\| h_{u(n,2)} G_{(n,2)} \right\|^2}{\lambda_{u(n,1)} P_n \left\| h_{u(n,2)} G_{(n,2)} \right\|^2 + P_D \left\| h_{pu(n,2)} \right\|^2 + \sigma_n^2}. \quad (15)$$

Event 3. The DU receiver only receives signals from the DU transmitter, whose SINR is denoted as γ_{D_p}:

$$\gamma_D = \frac{P_D \left\| h_{pp} \right\|^2}{\sigma_n^2}. \quad (16)$$

3.1. Outage Probability. In this section, we study the outage probability of *CU* and *DU*. The outage probability of the user 1, user 2, and *DU* is given by $P_1^{out}, P_2^{out}, P_D^{out}$:

$$\begin{aligned} P_1^{out} &= P\left(\log\left(1 + \gamma_{1 \longrightarrow 2}\right) < R_2 \ or \ \log\left(1 + \gamma_1\right) < R_1\right) \\ &= 1 \\ &\quad - P\left(\log\left(1 + \gamma_{1 \longrightarrow 2}\right) \geq R_2\right) P\left(\log\left(1 + \gamma_1\right) \geq R_1\right), \end{aligned} \quad (17)$$

$$P_2^{out} = P\left(\log\left(1 + \gamma_2\right) < R_2\right), \quad (18)$$

$$P_D^{out} = P\left(\log\left(1 + \gamma_D\right) < R_D\right), \quad (19)$$

where R_1, R_2, R_D are the target rates of user 1, user 2, and *DU*.

Firstly, we consider the outage probability of user 1 P_1^{out}; then $P(\log(1 + \gamma_{1 \longrightarrow 2}) \leq R_2)$ can be rewritten as $P(\gamma_{1 \longrightarrow 2} \leq 2^{R_2} - 1)$, so we set

$$F(m, a, b, c, d) = P\left(\frac{aH_1}{bH_1 + dH_2 + c} \leq m\right). \quad (20)$$

According to (13),(20), we can get

$$P\left(\gamma_{1\longrightarrow 2} \le 2^{R_2}-1\right) = F\left(m,a,b,c,d\right) = F_{\gamma_{1\longrightarrow 2}}\left(m\right), \quad (21)$$

where $a = \lambda_{u(n,2)}P_n\|G_{(n,1)}\|^2$, $b = \lambda_{u(n,1)}P_n\|G_{(n,1)}\|^2$, $d = P_D$, $c = \sigma_n^2, m = 2^{R_2}-1$, and $H_1 = \|h_{u(n,1)}\|^2 \sim Gamma(\omega,\psi)$, $H_2 = \|h_{pu(n,1)}\|^2 \sim Gamma(\eta,\theta)$; then

$$\begin{aligned} F_{\gamma_{1\longrightarrow 2}}\left(m\right) &= P\left(\frac{aH_1}{bH_1+dH_2+c} \le m\right) \\ &= \int_0^\infty P\left(\frac{ay}{by+dH_2+c} \le m\right) f_{H_1}\left(y\right)dy \\ &= \int_0^\infty P\left(\frac{ay-bmy-cm}{dm} \le H_2\right) f_{H_1}\left(y\right)dy. \end{aligned} \quad (22)$$

In order to determine if $(ay-bmy-cm)/dm \le 0$, we set $\Phi = cm/(a-bm)$. When $\Phi \le 0$, $(ay-bmy-cm)/dm \le 0$, so $P((ay-bmy-cm)/dm \le H_2) = 1$; therefore

$$F_{\gamma_{1\longrightarrow 2}}\left(m\right) = 1. \quad (23)$$

When $\Phi > 0$, which is $m < a/b$,

$$\begin{aligned} F_{\gamma_{1\longrightarrow 2}}\left(m\right) &= \int_0^\Phi f_{H_1}\left(y\right)dy \\ &+ \int_\Phi^\infty \left(1-F_{H_2}\left(\frac{ay-bmy-cm}{dm}\right)\right) f_{H_1}\left(y\right)dy \\ &= \int_\Phi^\infty \sum_{j=0}^{\eta-1}\frac{1}{j!\theta^j}\left(\frac{a-bm}{dm}y-\frac{c}{d}\right)^j \\ &\cdot e^{-(((a-bm)/dm\theta)y-c/d\theta)}\frac{1}{\psi^\omega\Gamma\left(\omega\right)}y^{\omega-1}e^{-y/\psi}dy \\ &+ \int_0^\Phi f_{H_1}\left(y\right)dy. \end{aligned} \quad (24)$$

We set $\alpha = (a-bm)/dm$, $\beta = -c/d$, and

$$\begin{aligned} F_{\gamma_{1\longrightarrow 2}}\left(m\right) &= \int_0^\Phi f_{H_1}\left(y\right)dy + \frac{1}{\psi^\omega\Gamma\left(\omega\right)}\sum_{j=0}^{\eta-1}\frac{1}{j!\theta^j} \\ &\cdot \int_\Phi^\infty \left(\alpha y+\beta\right)^j e^{-((\alpha/\theta)y+\beta/\theta)}y^{\omega-1}e^{-y/\psi}dy. \end{aligned} \quad (25)$$

As for $(x+a)^k = \sum_{j=0}^k \binom{k}{j} x^j a^{k-j}$, then

$$\begin{aligned} F_{\gamma_{1\longrightarrow 2}}\left(m\right) &= \frac{1}{\psi^\omega\Gamma\left(\omega\right)}\sum_{j=0}^{\eta-1}\frac{1}{j!\theta^j}\sum_{i=0}^{j}\binom{j}{i}\alpha^i\beta^{j-i}e^{-\beta/\theta} \\ &\cdot \int_\Phi^\infty \left(y\right)^{\omega+i-1}e^{-(\alpha/\theta+1/\psi)y}dy \\ &+ \int_0^\Phi f_{H_1}\left(y\right)dy. \end{aligned} \quad (26)$$

We set

$$J\left(a,n,x\right) = e^{ax}\sum_{k=0}^{n}\frac{(-1)^k\,k!\binom{n}{k}}{a^{k+1}}x^{n-k}. \quad (27)$$

Then by substituting (27) into (26), $F_{\gamma_{1\longrightarrow 2}}(m)$ can be denoted as

$$\begin{aligned} F_{\gamma_{1\longrightarrow 2}}\left(m\right) &= \frac{1}{\psi^\omega\Gamma\left(\omega\right)}\sum_{j=0}^{\eta-1}\frac{1}{j!\theta^j}\sum_{i=0}^{j}\binom{j}{i}\alpha^i\beta^{j-i}e^{-\beta/\theta} \\ &\cdot \left(-J\left(-\left(\frac{\alpha}{\theta}+\frac{1}{\psi}\right),\omega+j-1,\Phi\right)\right) \\ &+ \int_0^\Phi f_{H_1}\left(y\right)dy = \frac{1}{\psi^\omega\Gamma\left(\omega\right)}\sum_{j=0}^{\eta-1}\frac{1}{j!\theta^j} \\ &\cdot \sum_{i=0}^{j}\binom{j}{i}\alpha^i\beta^{j-i} \\ &\cdot e^{-\beta/\theta}\left(-J\left(-\left(\frac{\alpha}{\theta}+\frac{1}{\psi}\right),\omega+j-1,\Phi\right)\right) \\ &+ \frac{1}{\psi^\omega\Gamma\left(\omega\right)}\left(J\left(-\left(\frac{1}{\psi}\right),\omega-1,\Phi\right)\right. \\ &\left.- J\left(-\left(\frac{1}{\psi}\right),\omega-1,0\right)\right). \end{aligned} \quad (28)$$

Similarly, by adopting different parameters with a,b,c,d, which is shown in Table 1, we can obtain $F_{\gamma_{1\longrightarrow 2}}(m), F_{\gamma_1}(m), F_{\gamma_2}(m)$.

In addition, when $H_3 = \|h_{pp}\|^2 \sim Gamma(\omega,\phi)$, $P_D\|h_{pp}\|^2/\sigma_n^2 \sim Gamma(\omega,(P_D/\sigma_n^2)\phi)$. Hence $F_{\gamma_D}(m)$ is denoted as

$$F_{\gamma_D}\left(m\right) = 1-\sum_{J=0}^{\omega-1}\frac{1}{j!\left(\left(P_D/\sigma_n^2\right)\phi\right)^j}x^j e^{-x\sigma_n^2/P_D\phi}. \quad (29)$$

Finally, the outage probability of user 1, user 2, and *DU* can be evaluated by $F_{\gamma_{1\longrightarrow 2}}(m), F_{\gamma_1}(m), F_{\gamma_2}(m), F_{\gamma_D}(m)$, which are formulated as

$$\begin{aligned} P_1^{out} &= 1-\left(1-F_{\gamma_{1\longrightarrow 2}}\left(2^{R_2}-1\right)\right) \\ &\quad * \left(1-F_{\gamma_1}\left(2^{R_1}-1\right)\right), \end{aligned} \quad (30)$$

$$P_2^{out} = F_{\gamma_2}\left(2^{R_2}-1\right), \quad (31)$$

$$P_D^{out} = F_{\gamma_D}\left(2^{R_D}-1\right). \quad (32)$$

3.2. Ergodic Capacity. The ergodic capacity is the average capacity of channel which can be defined as the instantaneous end-to-end mutual information expectations and denoted as

$$\begin{aligned} C_{erg} &= \mathbb{E}\left[\log_2\left(1+\gamma_1\right)\right] + \mathbb{E}\left[\log_2\left(1+\gamma_2\right)\right] \\ &\quad + \mathbb{E}\left[\log_2\left(1+\gamma_D\right)\right]. \end{aligned} \quad (33)$$

Table 1: Parameters of the outage probability.

	a	b	c	d
$F_{\gamma_{1\longrightarrow 2}}(m)$	$\lambda_{u(n,1)}P_n\left\|G_{(n,1)}\right\|^2$	$\lambda_{u(n,2)}P_n\left\|G_{(n,2)}\right\|^2$	σ_n^2	P_D
$F_{\gamma_1}(m)$	$\lambda_{u(n,1)}P_n\left\|G_{(n,1)}\right\|^2$	0	σ_n^2	P_D
$F_{\gamma_2}(m)$	$\lambda_{u(n,2)}P_n\left\|G_{(n,2)}\right\|^2$	$\lambda_{u(n,1)}P_n\left\|G_{(n,1)}\right\|^2$	σ_n^2	P_D

The ergodic capacity of the system can be obtained by substituting (14), (15), and (16) into (33), which is formulated as

$$\begin{aligned}
C_{erg} &= \mathbb{E}\left[\log_2\left(1+\frac{\lambda_{u(n,1)}P_n\left\|h_{u(n,1)}G_{(n,1)}\right\|^2}{P_D\left\|h_{pu(n,1)}\right\|^2+\sigma_n^2}\right)\right] \\
&+\mathbb{E}\left[\log_2\left(1\right.\right. \\
&\left.\left.+\frac{\lambda_{u(n,2)}P_n\left\|h_{u(n,2)}G_{(n,2)}\right\|^2}{\lambda_{u(n,1)}P_n\left\|h_{u(n,2)}G_{(n,2)}\right\|^2+P_D\left\|h_{pu(n,2)}\right\|^2+\sigma_n^2}\right)\right]+\mathbb{E}[\log_2\left(1+\frac{P_D\left\|h_{pp}\right\|^2}{\sigma_n^2}\right) \\
&=\mathbb{E}\left[\log_2\left(1+\frac{\lambda_{u(n,1)}P_n\left\|G_{(n,1)}\right\|^2}{\sigma_n^2}\left\|h_{u(n,1)}\right\|^2+\frac{P_D}{\sigma_n^2}\left\|h_{pu(n,1)}\right\|^2\right)\right] \\
&-\mathbb{E}\left[\log_2\left(1+\frac{P_D}{\sigma_n^2}\left\|h_{pu(n,1)}\right\|^2\right)\right] \\
&+\mathbb{E}\left[\log_2\left(1+\left(\frac{\lambda_{u(n,2)}P_n\left\|G_{(n,2)}\right\|^2}{\sigma_n^2}\right.\right.\right. \\
&\left.\left.\left.+\frac{\lambda_{u(n,1)}P_n\left\|G_{(n,2)}\right\|^2}{\sigma_n^2}\right)\left\|h_{u(n,2)}\right\|^2+\frac{P_D}{\sigma_n^2}\left\|h_{pu(n,2)}\right\|^2\right)\right] \\
&-\mathbb{E}\left[\log_2\left(1+\frac{P_D}{\sigma_n^2}\left\|h_{pu(n,2)}\right\|^2+\left(\frac{\lambda_{u(n,1)}P_n\left\|G_{(n,2)}\right\|^2}{\sigma_n^2}\right)\right.\right. \\
&\left.\left.\cdot\left\|h_{u(n,2)}\right\|^2\right)\right]+\mathbb{E}\left[\log_2\left(1+\frac{P_D\left\|h_{pp}\right\|^2}{\sigma_n^2}\right)\right].
\end{aligned} \tag{34}$$

In order to compute (34), we first compute the first item of the formula. As we set before, $a=\lambda_{u(n,1)}P_n\|G_{(n,1)}\|^2$, $d=P_D$, $c=\sigma_n^2$, $H_1=\|h_{u(n,1)}\|^2\sim Gamma(\omega,\psi)$, $H_2=\|h_{pu(n,1)}\|^2\sim Gamma(\eta,\theta)$, we can get

$$\begin{aligned}
&\mathbb{E}\left[\log_2\left(1+\frac{\lambda_{u(n,1)}P_n\left\|G_{(n,1)}\right\|^2}{\sigma_n^2}\left\|h_{u(n,1)}\right\|^2\right.\right. \\
&\left.\left.+\frac{P_D}{\sigma_n^2}\left\|h_{pu(n,1)}\right\|^2\right)\right]=\mathbb{E}\left[\log_2(1+\frac{a}{c}H_1+\frac{d}{c}H_2\right].
\end{aligned} \tag{35}$$

According to the literature [43, 44], we can get

$$\mathbb{E}\left[\ln\left(1+x\right)\right]\approx\ln\left(1+\mathbb{E}\left[x\right]\right)-\frac{\mathbb{E}\left[x^2\right]-\left(\mathbb{E}\left[x\right]\right)^2}{2\left(1+\mathbb{E}\left[x\right]\right)^2}. \tag{36}$$

Based on (36), we start with $\mathbb{E}[x]$ and $\mathbb{E}[x^2]$, which can be written as

$$\begin{aligned}
&\mathbb{E}\left[\frac{a}{c}H_1+\frac{d}{c}H_2\right] \\
&=\int_0^\infty\int_0^\infty\left(\frac{a}{c}x+\frac{d}{c}y\right)f\left(x\right)f\left(y\right)dxdy \\
&=\int_0^\infty\left(\frac{a}{c}x\right)f\left(x\right)dx+\int_0^\infty\left(\frac{d}{c}y\right)f\left(y\right)dy \\
&=\frac{a}{c}\mathbb{E}\left(x\right)+\frac{d}{c}\mathbb{E}\left(y\right)=\frac{a}{c}\omega\psi+\frac{d}{c}\eta\theta,
\end{aligned} \tag{37}$$

$$\begin{aligned}
&\mathbb{E}\left[\left(\frac{a}{c}H_1+\frac{d}{c}H_2\right)^2\right] \\
&=\int_0^\infty\int_0^\infty\left(\frac{a}{c}x+\frac{d}{c}y\right)^2f\left(x\right)f\left(y\right)dxdy \\
&=\int_0^\infty\left(\frac{ax}{c}\right)^2f\left(x\right)dx+\int_0^\infty\left(\frac{dy}{c}\right)^2f\left(y\right)dy \\
&\quad+\int_0^\infty\int_0^\infty\frac{2adxy}{c^2}f\left(x\right)f\left(y\right)dxdy \\
&=\left(\frac{a^2}{c^2}\right)(\omega+1)\,\omega\left(\psi\right)^2+\left(\frac{d^2}{c^2}\right)(\eta+1)\,\eta\left(\theta\right)^2 \\
&\quad+\frac{2a\mathrm{d}}{c^2}\omega\eta\psi\theta.
\end{aligned} \tag{38}$$

By substituting (37) and (38) into (35), we can obtain the first item of formula (34), which can be denoted as

$$\begin{aligned}
&\mathbb{E}\left[\log_2\left(1+\frac{a}{c}H_1+\frac{d}{c}H_2\right)\right]=\log_2\left(e\right) \\
&\cdot\left(\ln\left(1+\frac{a}{c}\omega\psi+\frac{d}{c}\eta\theta\right)\right. \\
&\left.-\frac{\left(a^2/c^2\right)\omega\left(\psi\right)^2+\left(d^2/c^2\right)\eta\left(\theta\right)^2}{2\left(1+\left(a/c\right)\omega\psi+\left(d/c\right)\eta\theta\right)^2}\right).
\end{aligned} \tag{39}$$

Similarly, we can set a, b, c, d as different parameters to obtain the other items of the formula (34) and then pull everything together. The asymptotic result for the ergodic capacity of the consider system can be obtained.

4. Numerical Results

In this section, the outage probability and the ergodic capacity of MIMO-NOMA mmWave cellular network with D2D communications are investigated. The effects of different parameters on the probability of outage and ergodic capacity are analyzed such as the base station transmission power, the number of base station antennas, the power ratio of NOMA user, and the distance between D2D users. In order to verify the performance of the system, the traditional TDMA theme is adopted as the comparison between the two users of each beam. In particular, the time slot is equally divided by the two users. Hence the capacity of this theme is R_{TDMA}, which is denoted as

$$R_{TDMA} = \frac{1}{2}\left(\log\left(1+\gamma_1\right)+\log\left(1+\gamma_2\right)\right). \quad (40)$$

A simplified cellular network system is discussed for the performance analyzed here. The carrier frequency is 28GHz which is commonly used for wireless broadband service. There are 16 antennas in the base station whose coverage radius is 100m. There is single antenna with D2D user. And the distance between D2D users is 30m. Meanwhile, the transmission power of base station and D2D users is 5 dbm. In addition, there are 8 NOMA users and 4 D2D users in the cellular network. The path loss exponent is set as 3. Furthermore, the small scale fading is denoted as $H \sim Gamma(2,1)$ which is simplified for the simulation.

4.1. Outage Probability. In this section, we consider the outage probability of the NOMA far user and near user.

Figure 2 depicts the outage probability in the different base station transmission power with R_1 = 5 bit/s/Hz and R_2 = 3.32 bit/s/Hz. As the base station transmission power increases, it can be seen that the outage probability of the NOMA users decreases with the exponential form. Furthermore, the performance of each user's outage probability in the NOMA scheme is significantly better than the TDMA, and the closed-form solution obtained is consistent with the Monte Carlo simulation results.

In Figure 3, the impact of antenna number in the base station on the outage probability (R_1 = 5.64 bit/s/Hz and R_2 = 4 bit/s/Hz) is presented. The simulation results effectively verify that the number of antennas of the base station can decrease the users' outage probability in the MIMO-NOMA mmWave cellular network, thereby improving the throughput of the system under the limited time-frequency resources. As can be seen from Figure 3, the number of antennas has a greater impact on user 2 than user 1. When the number of antennas is 36, the outage probability of the system is satisfied which can balance the number of RF chains and the system performance. Then the NOMA scheme performs better than the traditional TDMA in the mmWave MIMO cellular network with D2D communications.

In Figure 4, we discuss the influence of the power ratio coefficient in the cellular network between the NOMA users. It can be seen that the outage probability (R_1 = 4 bit/s/Hz and R_2 = 3 bit/s/Hz) of the two users in NOMA is balanced when the power ratio coefficient is approximately 0.2.

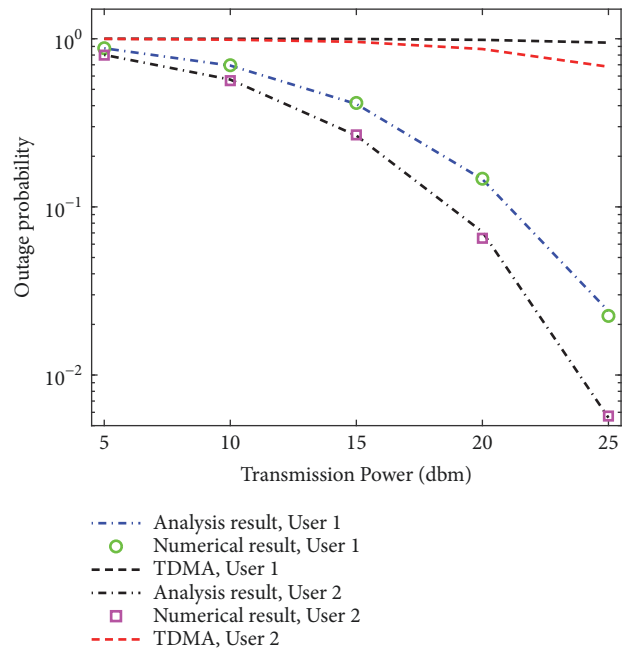

Figure 2: Impact of transmission power on outage probability.

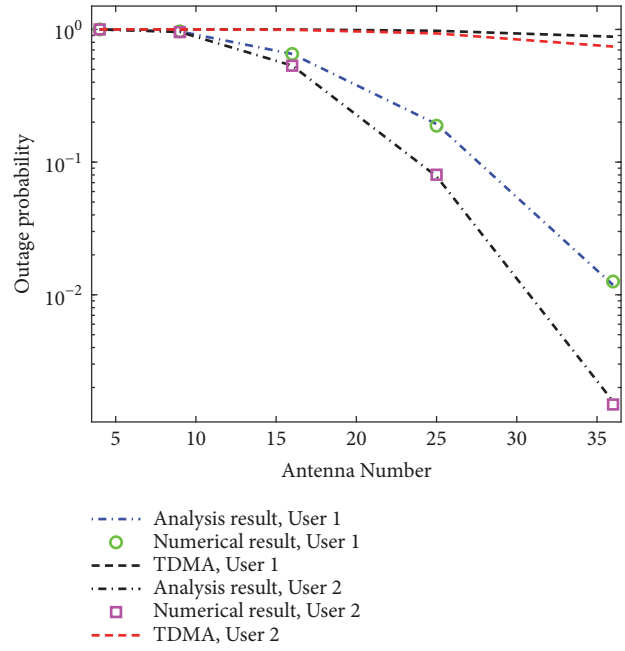

Figure 3: Impact of antenna number on outage probability.

In Figure 5, the effect of the distance between D2D users is considered. The figure indicates that the outage probability (R_1 = 5 bit/s/Hz and R_2 = 3.32 bit/s/Hz) of the NOMA users is reduced in the form of an exponent when the distance of D2D user is linear growth. Since the distance between D2D users is increasing, the interference from the D2D transmitter to the NOMA user is weak. Hence, the throughput of the NOMA users is improved, while the outage probability is dropping.

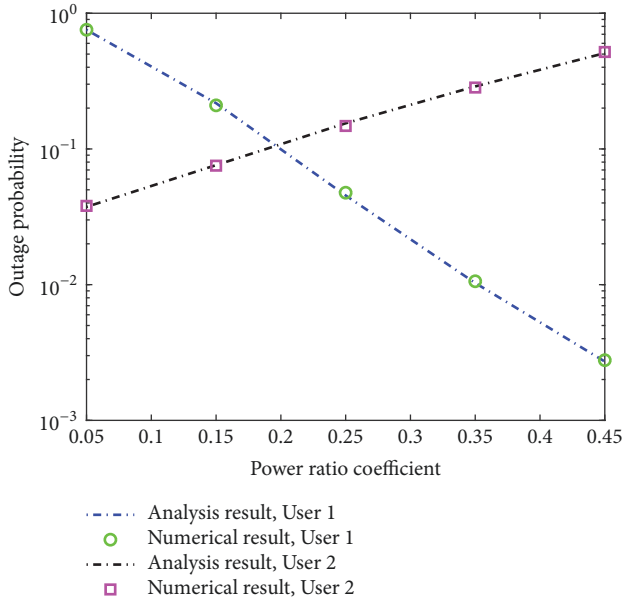

Figure 4: Impact of power ratio coefficient on outage probability.

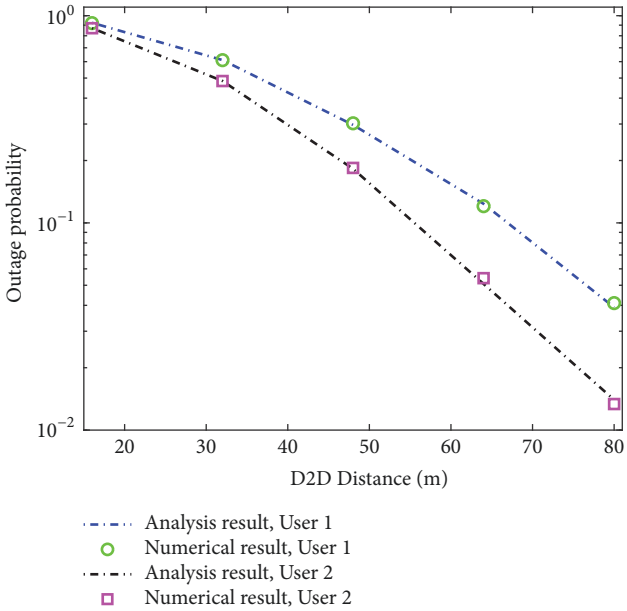

Figure 5: Impact of D2D distance on outage probability.

4.2. Ergodic Capacity. In this section, the total ergodic capacity is considered in the MIMO-NOMA mmWave cellular network with D2D communications. It can be seen that the numerical results are consistent with the closed-form solution which is better than the traditional TDMA. Meanwhile, the transmission power and the number of base station antennas have a greater impact, and the power ratio coefficient and the distance between D2D users have less effect.

In Figure 6, the impact of the transmission power of base station on the ergodic capacity is considered in the MIMO-NOMA mmWave cellular network with D2D communications. It is shown that the ergodic capacity is growing linearly

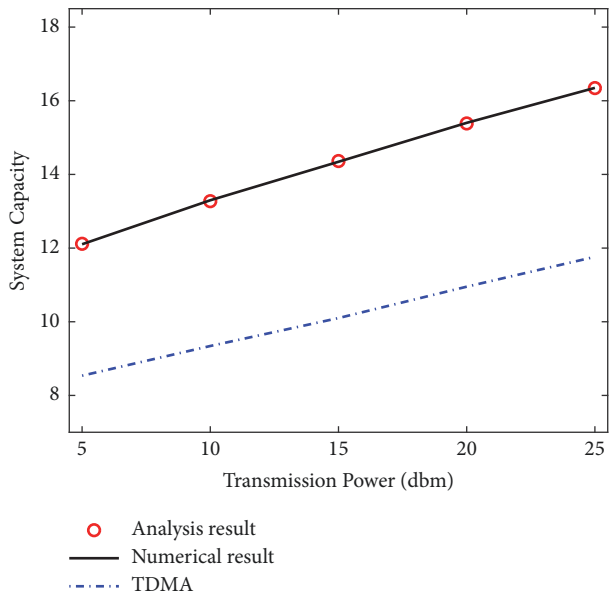

Figure 6: Impact of transmission power on ergodic capacity.

with the increase of transmission power. In addition, the ergodic capacity of the system we proposed is higher than the traditional TDMA. Hence, in order to improve the ergodic capacity of the system, we can increase the base station transmission power as much as possible without affecting others.

As the number of the base station antennas is increasing, it is indicated that the ergodic capacity can be improved better than the traditional TDMA in Figure 7. Benefiting from the length of mmWave, more and more antennas can be equipped for the base station. At the same time, we need to balance the improvement in ergodic capacity brought by the increasing of the number of antennas and the power consumption and hardware requirements of the increase in RF chains to determine the final number of antennas.

In Figure 8, the ergodic capacity is affected by the change of the power ratio coefficient of the NOMA users in the MIMO-NOMA mmWave cellular network with D2D communications. It can be seen that the total ergodic capacity changes slowly with the increase of power ratio.

In Figure 9, since the interference from the D2D users is decreasing, the total ergodic capacity is improved with the increase of the distance between the D2D users in the MIMO-NOMA mmWave cellular network. It can also be seen that the ergodic capacity in the MIMO-NOMA mmWave cellular network is always better than the traditional TDMA.

5. Conclusion

In this paper, the outage probability and the ergodic capacity of the NOMA in the MIMO-NOMA mmWave cellular network with D2D communications are studied. The closed-form solutions of the outage probability and the ergodic capacity are obtained, which are consistent with the numerical results. Meanwhile, the performance of NOMA is shown

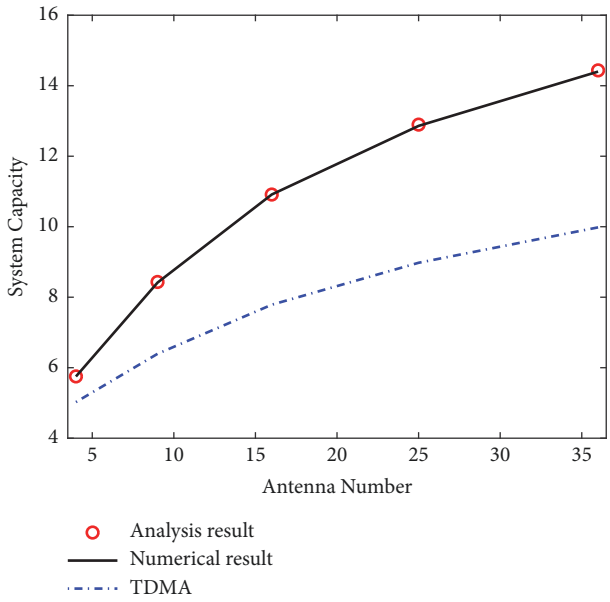

Figure 7: Impact of antenna number on ergodic capacity.

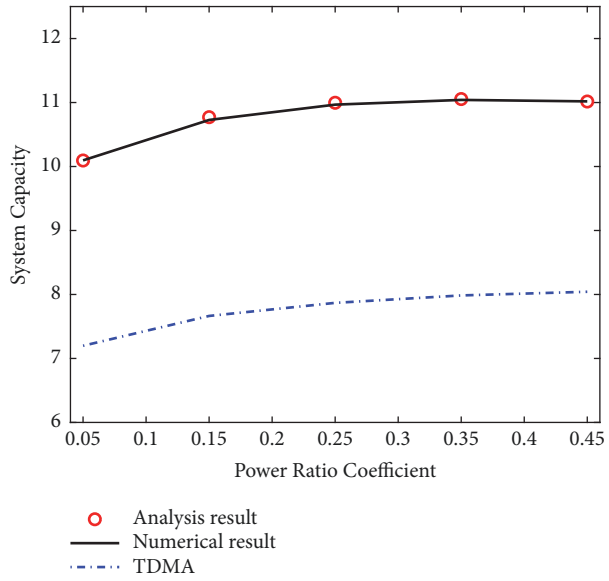

Figure 8: Impact of power ratio coefficient on ergodic capacity.

to be better than traditional TDMA in the MIMO mmWave cellular network with D2D communications. Furthermore, the higher transmission power of base station and the larger antenna array can also improve system performance.

Data Availability

No data were used to support this study.

Conflicts of Interest

The authors declare that there are no conflicts of interest regarding the publication of this paper.

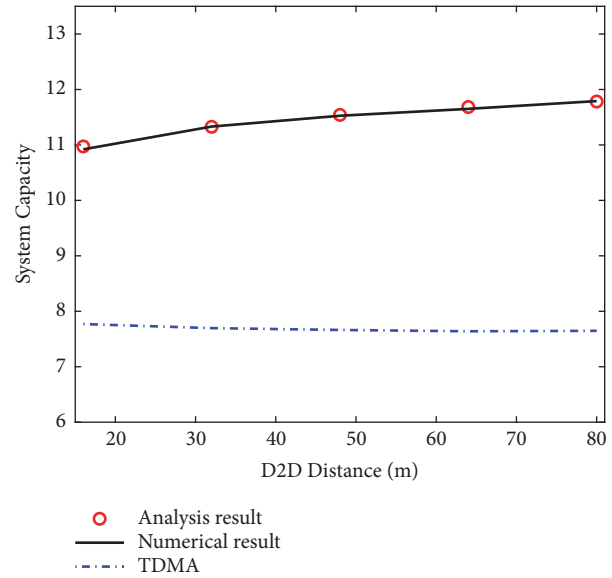

Figure 9: Impact of D2D distance on ergodic capacity.

Acknowledgments

This work was supported by Advance Research Projects of 13th Five-Year Plan of Civil Aerospace Technology (B0105) and the National Natural Science Foundation of China (61771051).

References

[1] M. Tehrani, M. Uysal, and H. Yanikomeroglu, "Device-to-device communication in 5G cellular networks: challenges, solutions, and future directions," *IEEE Communications Magazine*, vol. 52, no. 5, pp. 86–92, 2014.

[2] S.-Y. Lien, C.-C. Chien, G. S.-T. Liu, H.-L. Tsai, R. Li, and Y. J. Wang, "Enhanced LTE device-to-device proximity services," *IEEE Communications Magazine*, vol. 54, no. 12, pp. 174–182, 2016.

[3] L. Lei, Z. D. Zhong, C. Lin, and X. M. Shen, "Operator controlled device-to-device communications in LTE-advanced networks," *IEEE Wireless Communications Magazine*, vol. 19, no. 3, pp. 96–104, 2012.

[4] A. Asadi and V. Mancuso, "Network-assisted outband D2D-clustering in 5G cellular networks: theory and practice," *IEEE Transactions on Mobile Computing*, vol. 16, no. 8, pp. 2246–2259, 2017.

[5] J. Hu, W. Heng, Y. Zhu, G. Wang, X. Li, and J. Wu, "Overlapping coalition formation games for joint interference management and resource allocation in D2D communications," *IEEE Access*, vol. 6, pp. 6341–6349, 2018.

[6] H. Min, J. Lee, S. Park, and D. Hong, "Capacity enhancement using an interference limited area for device-to-device uplink underlaying cellular networks," *IEEE Transactions on Wireless Communications*, vol. 10, no. 12, pp. 3995–4000, 2011.

[7] Z. Uykan and R. Jantti, "Transmission-order optimization for bidirectional device-to-device (D2D) communications underlaying cellular TDD networks—a graph theoretic approach," *IEEE Journal on Selected Areas in Communications*, vol. 34, no. 1, pp. 1–14, 2016.

[8] L. L. Wei, R. Q. Hu, T. He, and Y. Qian, "Device-to-device(d2d) communications underlaying MU-MIMO cellular networks," in *Proceedings of the IEEE Global Communications Conference (GLOBECOM '13)*, pp. 4902–4907, IEEE, Atlanta, Ga, USA, December 2013.

[9] X. Li, W. Zhang, H. Zhang, and W. Li, "A combining call admission control and power control scheme for D2D communications underlaying cellular networks," *China Communications*, vol. 13, no. 10, pp. 137–145, 2016.

[10] H. Sun, Y. Xu, and R. Q. Hu, "A NOMA and MU-MIMO supported cellular network with underlaid D2D communications," in *Proceedings of the 2016 IEEE 83rd Vehicular Technology Conference (VTC Spring)*, pp. 1–5, Nanjing, China, May 2016.

[11] Z. Ding, X. Lei, G. K. Karagiannidis, R. Schober, J. Yuan, and V. K. Bhargava, "A survey on non-orthogonal multiple access for 5G networks: research challenges and future trends," *IEEE Journal on Selected Areas in Communications*, vol. 35, no. 10, pp. 2181–2195, 2017.

[12] N. Ye, X. Li, H. Yu, A. Wang, W. Liu, and X. Hou, "Deep learning aided grant-free noma towards reliable low-latency access in tactile internet of things," *IEEE Transactions on Industrial Informatics*, vol. 15, no. 5, pp. 2995–3005, 2019.

[13] J. An, K. Yang, J. Wu, N. Ye, S. Guo, and Z. Liao, "Achieving sustainable ultra-dense heterogeneous networks for 5G," *IEEE Communications Magazine*, vol. 55, no. 12, pp. 84–90, 2017.

[14] N. Ye, A. Wang, X. Li, H. Yu, A. Li, and H. Jiang, "A random non-orthogonal multiple access scheme for mmtc," in *Proceedings of the 2017 IEEE 85th Vehicular Technology Conference (VTC Spring)*, pp. 1–6, June 2017.

[15] K. Yang, N. Yang, N. Ye, M. Jia, Z. Gao, and R. Fan, "Non-orthogonal multiple access: achieving sustainable future radio access," *IEEE Communications Magazine*, vol. 57, no. 2, pp. 116–121, 2019.

[16] S. M. R. Islam, N. Avazov, O. A. Dobre, and K.-S. Kwak, "Power-domain non-orthogonal multiple access (NOMA) in 5G systems: potentials and challenges," *IEEE Communications Surveys & Tutorials*, vol. 19, no. 2, pp. 721–742, 2017.

[17] N. Ye, A. Wang, X. Li, W. Liu, X. Hou, and H. Yu, "On constellation rotation of noma with sic receiver," *IEEE Communications Letters*, vol. 22, no. 3, pp. 514–517, 2018.

[18] M. Hojeij, C. A. Nour, J. Farah, and C. Douillard, "Joint resource and power allocation technique for downlink power-domain non-orthogonal multiple access," in *Proceedings of the 2018 IEEE Conference on Antenna Measurements & Applications (CAMA)*, pp. 1–4, September 2018.

[19] F. A. Rabee, K. Davaslioglu, and R. Gitlin, "The optimum received power levels of uplink non-orthogonal multiple access (NOMA) signals," in *Proceedings of the 18th IEEE Wireless and Microwave Technology Conference, WAMICON 2017*, pp. 1–4, USA, April 2017.

[20] Y. Li and G. A. A. Baduge, "Noma-aided cell-free massive mimo systems," *IEEE Wireless Communications Letters*, vol. 7, pp. 950–953, 2018.

[21] N. Ye, A. Wang, X. Li et al., "Rate-adaptive multiple access for uplink grant-free transmission," *Wireless Communications and Mobile Computing*, vol. 2018, Article ID 8978207, 21 pages, 2018.

[22] N. Ye, H. Han, L. Zhao, and A.-H. Wang, "Uplink nonorthogonal multiple access technologies toward 5G: a survey," *Wireless Communications and Mobile Computing*, vol. 2018, Article ID 6187580, 26 pages, 2018.

[23] Y. Liu, W.-J. Lu, S. Shi et al., "Performance analysis of a downlink cooperative noma network over nakagami-m fading channels," *IEEE Access*, vol. 6, pp. 53034–53043, 2018.

[24] X. Wang, J. Wang, L. He, and J. Song, "Outage analysis for downlink noma with statistical channel state information," *IEEE Wireless Communications Letters*, vol. 7, no. 2, pp. 142–145, 2018.

[25] A. J. Paulraj, D. A. Gore, R. U. Nabar, and H. Bölcskei, "An overview of MIMO communications—a key to gigabit wireless," *Proceedings of the IEEE*, vol. 92, no. 2, pp. 198–217, 2004.

[26] W. Cai, C. Chen, L. Bai, Y. Jin, and J. Choi, "User selection and power allocation schemes for downlink NOMA systems with imperfect CSI," in *Proceedings of the 2016 IEEE 84th Vehicular Technology Conference (VTC-Fall)*, pp. 1–5, Montreal, QC, Canada, September 2016.

[27] Z. Ding and H. V. Poor, "Design of massive-MIMO-NOMA with limited feedback," *IEEE Signal Processing Letters*, vol. 23, no. 5, pp. 629–633, 2016.

[28] Z. Ding, F. Adachi, and H. V. Poor, "The application of MIMO to non-orthogonal multiple access," *IEEE Transactions on Wireless Communications*, vol. 15, no. 1, pp. 537–552, 2016.

[29] Q. Sun, S. Han, I. Chin-Lin, and Z. Pan, "On the ergodic capacity of MIMO NOMA systems," *IEEE Wireless Communications Letters*, vol. 4, no. 4, pp. 405–408, 2015.

[30] J. Ding, J. Cai, and C. Yi, "An improved coalition game approach for MIMO-NOMA clustering integrating beamforming and power allocation," *IEEE Transactions on Vehicular Technology*, vol. 68, no. 2, pp. 1672–1687, 2019.

[31] J.-B. Kim, I.-H. Lee, and J. Lee, "Capacity scaling for D2D aided cooperative relaying systems using NOMA," *IEEE Wireless Communications Letters*, vol. 7, no. 1, pp. 42–45, 2018.

[32] S. Papaioannou, G. Kalfas, C. Vagionas et al., "5G mm Wave Networks Leveraging Enhanced Fiber-Wireless Convergence for High-Density Environments: The 5G-PHOS Approach," in *Proceedings of the 2018 IEEE International Symposium on Broadband Multimedia Systems and Broadcasting (BMSB)*, pp. 1–5, Valencia, Spain, June 2018.

[33] S. A. Naqvi and S. A. Hassan, "Combining NOMA and mmWave technology for cellular communication," in *Proceedings of the 2016 IEEE 84th Vehicular Technology Conference (VTC-Fall)*, pp. 1–5, Montreal, QC, Canada, September 2016.

[34] F. Rusek, D. Persson, B. K. Lau et al., "Scaling up MIMO: opportunities and challenges with very large arrays," *IEEE Signal Processing Magazine*, vol. 30, no. 1, pp. 40–60, 2013.

[35] T. Bai, A. Alkhateeb, and R. W. Heath, "Coverage and capacity of millimeter-wave cellular networks," *IEEE Communications Magazine*, vol. 52, no. 9, pp. 70–77, 2014.

[36] X. Gao, L. Dai, S. Han, I. Chih-Lin, and R. W. Heath, "Energy-efficient hybrid analog and digital precoding for MmWave MIMO systems with large antenna arrays," *IEEE Journal on Selected Areas in Communications*, vol. 34, no. 4, pp. 998–1009, 2016.

[37] X. Gao, L. Dai, Z. Chen, Z. Wang, and Z. Zhang, "Near-optimal beam selection for beamspace mmwave massive mimo systems," *IEEE Communications Letters*, vol. 20, no. 5, pp. 1054–1057, 2016.

[38] Z. Wang, M. Li, Q. Liu, and A. L. Swindlehurst, "Hybrid precoder and combiner design with low-resolution phase shifters in mmWave MIMO systems," *IEEE Journal of Selected Topics in Signal Processing*, vol. 12, no. 2, pp. 256–269, 2018.

[39] Y. Sun, Z. Ding, and X. Dai, "On the performance of downlink NOMA in multi-cell mmWave networks," *IEEE Communications Letters*, vol. 22, no. 11, pp. 2366–2369, 2018.

[40] N. Deng and M. Haenggi, "A fine-grained analysis of millimeter-wave device-to-device networks," *IEEE Transactions on Communications*, vol. 65, no. 11, pp. 4940–4954, 2017.

[41] D. Zhang, Z. Zhou, C. Xu, Y. Zhang, J. Rodriguez, and T. Sato, "Capacity analysis of NOMA with mmWave massive MIMO systems," *IEEE Journal on Selected Areas in Communications*, vol. 35, no. 7, pp. 1606–1618, 2017.

[42] S. Singh, M. N. Kulkarni, A. Ghosh, and J. G. Andrews, "Tractable model for rate in self-backhauled millimeter wave cellular networks," *IEEE Journal on Selected Areas in Communications*, vol. 33, no. 10, pp. 2191–2211, 2015.

[43] X. Yan, H. Xiao, C.-X. Wang, and K. An, "On the ergodic capacity of NOMA-based cognitive hybrid satellite terrestrial networks," in *Proceedings of the 2017 IEEE/CIC International Conference on Communications in China, ICCC 2017*, pp. 1–5, China, October 2017.

[44] Y. Huang, F. Al-Qahtani, C. Zhong, Q. Wu, J. Wang, and H. Alnuweiri, "Performance analysis of multiuser multiple antenna relaying networks with co-channel interference and feedback delay," *IEEE Transactions on Communications*, vol. 62, no. 1, pp. 59–73, 2014.